THE JOURNAL OF PHYSICAL CHEMISTRY B

Article

pubs.acs.org/JPCB

Ultrafast Excited-State Intramolecular Proton Transfer of Aloesaponarin I

Shin-ichi Nagaoka,[†] Hidemitsu Uno,[†] and Dan Huppert*[,‡]

[†]Department of Chemistry, Faculty of Science and Graduate School of Science and Engineering, Ehime University, Matsuyama 790-8577, Japan

[‡]Raymond and Beverly Sackler Faculty of Exact Sciences, School of Chemistry, Tel Aviv University, Tel Aviv 69978, Israel

Supporting Information

ABSTRACT: Time-resolved emission of aloesaponarin I was studied with the fluorescence up-conversion and time-correlated single-photon-counting techniques. The rates of the excited-state intramolecular proton transfer, of the solvent and molecular rearrangements, and of the decay from the excited proton-transferred species were determined and interpreted in the light of time-dependent density functional calculations. These results were discussed in conjunction with UV protection and singlet-oxygen quenching activity of aloe.

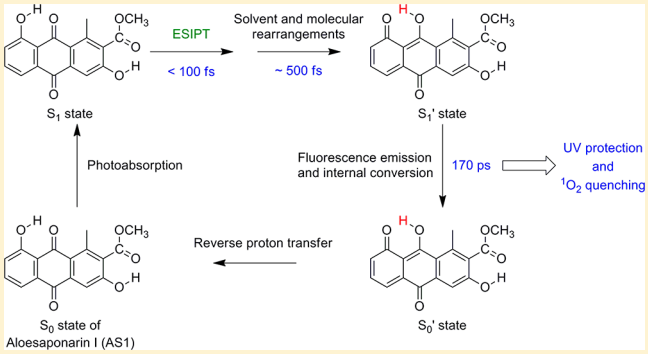

1. INTRODUCTION

Cosmetic and healing properties of aloe have been valued for thousands of years.[1−5] Legend has it that use of aloe was an important part of the beauty regime of the Egyptian queens, Nefertiti and Cleopatra.[6] Nowadays, aloe extract is used all over the world as an active ingredient in hundreds of sun blocks (UV protectors), skin lotions, and cosmetics. Given the substantial solar flux in Egypt,[7] protection from the sun would be very important, and the UV protective activity of aloe may have maintained the beauty of Cleopatra of Greek ancestry[8] in her occasional going out of her palace. This paper focuses on the UV protective activity of aloesaponarin I (methyl 3,8-dihydroxy-1-methyl-9,10-dioxo-9,10-dihydroanthracene-2-carboxylate, AS1 in Chart 1) found in aloe.

UV protection by a molecule is performed by rapid regeneration of the ground electronic state (S_0) following efficient UV absorption through fast nonradiative relaxation without triplet photosensitization.[9,10] Accordingly, the fast nonradiative relaxation from the lowest-excited singlet state (S_1) to the S_0 state (internal conversion) causing the UV protection is thought to occur in some chemical constituents found in aloe. The fast internal conversion occurs only under special conditions such as excited-state intramolecular proton transfer (ESIPT) through a hydrogen bond,[11−15] cis−trans isomerization, etc., because usual $S_1 \rightarrow S_0$ internal conversion is much slower than fluorescence and intersystem crossing to triplet states (Ermolev's rule).[16] Since aloe contains various intramolecularly hydrogen-bonded molecules including chemical constituents characteristics of aloe (AS1, aloe-emodin, aloin, etc.),[17] the above-mentioned special condition causing its UV protection would mainly be ESIPT.

Chart 1. Structures of Aloesaponarin I (AS1) and Related Molecules Used in the Present Work[a]

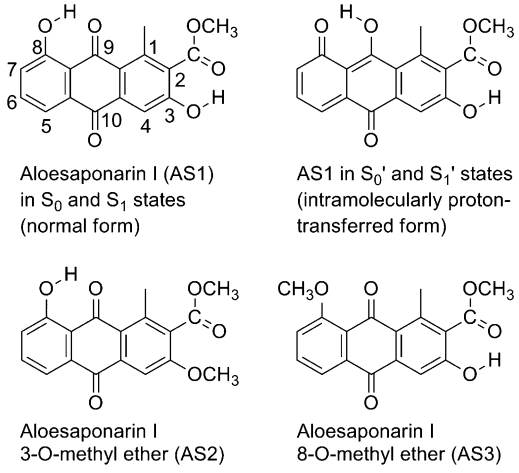

[a]For AS1, the structures in the S_0 (S_1) and S_0' (S_1') states are shown (normal and intramolecularly proton-transferred forms, respectively).

In molecules susceptible to ESIPT, photoexcitation of the normal form (stable S_0-state species) produces the lowest-excited $^1(\pi,\pi^*)$ state (S_1), in which ESIPT along an intramolecular hydrogen bond takes place rapidly, stabilizing

Special Issue: Paul F. Barbara Memorial Issue

Received: July 11, 2012
Revised: November 15, 2012
Published: November 15, 2012

the S_1 state (Figure 1).[11−15] The lowest-excited singlet state of the intramolecularly proton-transferred form (S_1') decays to its

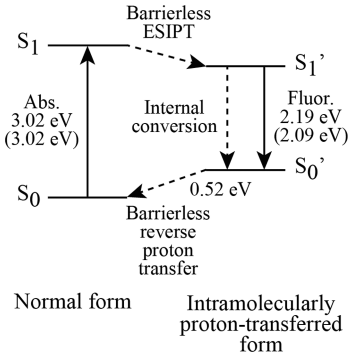

Figure 1. Potential energy levels of S_0, S_1, S_0', and S_1' states of an ESIPT-susceptible molecule such as AS1. "Abs." and "Fluor." denote photoabsorption and fluorescence, respectively. The values given in the figure show the computational transition energies of AS1 models (Chart 2) at the B3LYP/6-311G**//LC-BLYP/6-311G** level. The corresponding experimental values are given in the parentheses.

ground state (S_0') through fluorescence or the above-mentioned internal conversion,[18] which is so fast as to dominate over the photosensitization at room temperature. Then, $S_0' \rightarrow S_0$ reverse proton transfer takes place and the stable normal form is regenerated. These ESIPT phenomena are consistent with the explanation that the nodal plane of the wave function stabilizes the proton-transferred form in the S_1' state (nodal plane model).[19−22] Because a significant amount of absorption photon energy is dissipated as heat in the cycle given in Figure 1, the proton-transferred form fluoresces at a lower energy with an unusually large Stokes shift (solid and broken curves in Figure 2). The whole fast energy dissipation

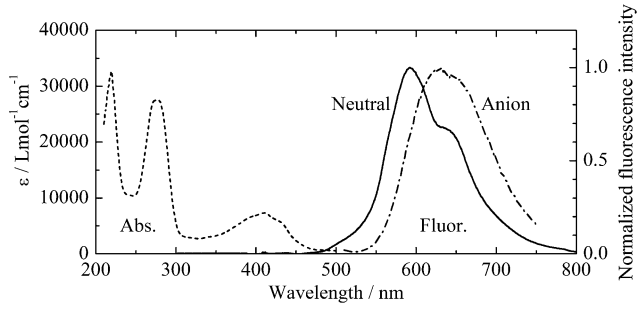

Figure 2. Absorption (Abs.) and fluorescence (Fluor.) spectra of AS1 in EtOH (broken and solid curves, respectively)[33] and fluorescence spectrum of AS1 in a basic EtOD solution (alternate long-and-short dashed curve) at room temperature. The fluorescence spectra in EtOH and basic EtOD were obtained by photoexcitation at 400 and 500 nm, respectively, and have not been corrected for the spectral sensitivity of the detector.

caused by ESIPT prevents the harmful photosensitization and provides the UV protection[10] together with resistance to UV degradation of the molecule itself. The regenerated normal form can contribute again to the ESIPT-based UV protection. As suggested previously,[23,24] out-of-plane bending and/or torsional motion around the intramolecular hydrogen bond play an important role in the fast $S_1' \rightarrow S_0'$ internal conversion at room temperature. When the ESIPT is blocked, the photochemical stability is greatly reduced[25] by enhancement of the photosensitization through the intersystem crossing, which is very fast in quinones without intramolecular hydrogen bonding (skeletal molecules of AS1).[26,27] Various intramolecularly hydrogen-bonded molecules susceptible to ESIPT are widely used as UV protectors (see ref 28a and many references cited in ref 29). Some intramolecularly hydrogen-bonded molecules found in aloe could also be useful as the UV protector with ESIPT.

One of the chemical constituents found in aloe is AS1, which has two intramolecular hydrogen bonds.[30−32] Nagaoka et al.[33,34] previously found that AS1 has UV protection and singlet oxygen ($^1O_2$, $^1\Delta_g$ state) quenching activity, and the UV protective activity provided by ESIPT in AS1 and the related molecules correlates with their $^1O_2$ quenching activity. The ESIPT of AS1 takes place along only one of the molecule's two intramolecular hydrogen bonds (O_8—H_8···O_9=C_9), which can be understood by considering the nodal plane model.[19−22,33]

However, details of the ESIPT of AS1 have not yet been elucidated. Especially, the rates of the ESIPT and of the decay from the S_1' state are unknown. Accordingly, in the present paper, we have studied the ESIPT of AS1 by means of ultrafast spectroscopy and time-dependent density functional theory (TDDFT), and the results have been discussed in conjunction with the UV protection and $^1O_2$ quenching activity of aloe.

2. EXPERIMENTAL SECTION

Preparation methods and analytical data of AS1, aloesaponarin I 3-*O*-methyl ether (methyl 8-hydroxy-3-methoxy-1-methyl-9,10-dioxo-9,10-dihydroanthracene-2-carboxylate, AS2), and aloesaponarin I 8-*O*-methyl ether (methyl 3-hydroxy-8-methoxy-1-methyl-9,10-dioxo-9,10-dihydroanthracene-2-carboxylate, AS3) (Chart 1) were reported in previous papers.[31−33] The solvents used for our spectral measurements were commercially available and used without further purification.

The fluorescence up-conversion technique was employed in this study to measure time-resolved emission of AS1 at room temperature. The laser used for the fluorescence up-conversion was a cavity dumped Ti:sapphire femtosecond laser (Mira, Coherent), which provided short pulses (150 fs) at around 800 nm.[35] The cavity dumper operated with a relatively low repetition rate of 800 kHz, and the up-conversion system (FOG-100, CDP, Russia) also operated at 800 kHz. The samples were excited by pulses of ∼8 mW on average at the second-harmonic-generation (SHG) frequency (∼400 nm). The time response of the up-conversion system was evaluated by measuring the relatively strong Raman−Stokes line of water shifted by 3600 cm^{-1}. It was found that the full width at half-maximum (fwhm) of the signal was 300 fs, which enabled us to observe decay times longer than 100 fs. If the decay component is longer than 200 fs, and it is not followed by a second longer decay with an amplitude of ∼10%, then the decay time component's amplitude observed will be ≥90%. In that case, the decay time can be accurately determined within an error margin of 10%. The samples were placed in a rotating optical cell to avoid degradation. We found that, during our time-resolved measurements in the cell rotating at a frequency of 10 Hz, degradation of the sample was marginal, and had no effect on the signal's decay profile.

Time-resolved fluorescence experiments at low temperatures were performed with the time-correlated single-photon-counting (TCSPC) technique.[36] The TCSPC detection system was based on a Hamamatsu 3809U photomultiplier (PM), which collected the fluorescence that had been spectrally

dx.doi.org/10.1021/jp306870y | J. Phys. Chem. B 2013, 117, 4347−4353

selected by a double monochromator operating in the nondispersive mode with a spectral width of 10 nm. The PM output was processed by an Edinburgh Instruments TCC 900 computer module for TCSPC. The overall instrumental-response function was about 40 ps in fwhm. The excitation-pulse energy of the above-mentioned laser operating at the SHG frequency was reduced to about 10 pJ through some neutral-density filters. The temperature of the sample was controlled by placing the sample in a liquid-N_2 cryostat with a thermal stability of approximately ±1.5 K.

3. COMPUTATIONAL METHOD AND PROCEDURE

The experimental results on ESIPT of AS1 were interpreted in light of TDDFT calculations of models for the normal and intramolecularly proton-transferred forms (Chart 2). Note that

Chart 2. Molecular Structures of Models for Normal and Intramolecularly Proton-Transferred Forms of AS1[a]

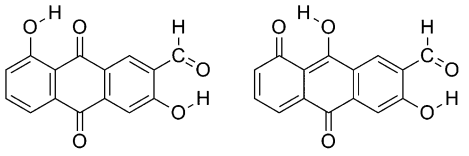

[a]These models are used in the present computational work.

the ESIPT takes place along only one of the molecule's two intramolecular hydrogen bonds (O_8—H_8···O_9═C_9), as shown in Chart 2.[33] It is known that the TDDFT calculation with the B3LYP functional satisfactorily reproduces experimental electronic transition energies of ESIPT-susceptible molecules.[15,37] However, it drastically underestimates the energies of charge transfer (CT) states in excited-state proton transfer, resulting in a wrong picture that many CT states are included in low-lying excited states.[38] In contrast, the long-range corrected TDDFT method such as LC-BLYP exhibits no CT state in the low-lying excited states.[38] The 6-311G** basis set is widely used in ab initio molecular orbital calculations.[39] Accordingly, the present calculations were done at the time-dependent B3LYP/6-311G**//LC-BLYP/6-311G** level using the Gaussian 09 program.[40] The optimized structures in the ground and lowest-excited $^1(\pi,\pi^*)$ states are given in the Supporting Information, together with the computational results at the time-dependent LC-BLYP/6-311G**//B3LYP/6-311G** level.

4. RESULTS AND DISCUSSION

Time-resolved emission signals of AS1, AS2, and AS3 at room temperature were obtained with the fluorescence up-conversion technique. All of the fluorescence rise-and-decay signals obtained are given in the Supporting Information, together with the decay signals obtained with the TCSPC technique and $S_1' \rightarrow S_0'$ fluorescence lifetimes of AS1 at various temperatures. For reference, the absorption and fluorescence spectra of AS1 in ethanol (EtOH) are shown in Figure 2.[33]

Figure 3 shows some fluorescence rise-and-decay signals of AS1 monitored between 470 and 650 nm in EtOH at room temperature. As the monitoring wavelength increases, the fluorescence rise and decay become slower. In the fluorescence of AS1, the range of $\lambda \leq 520$ nm is most likely the fluorescence

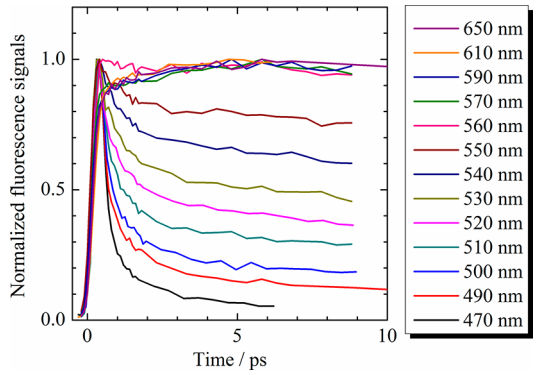

Figure 3. Fluorescence rise-and-decay signals of AS1 monitored between 470 and 650 nm in EtOH at room temperature.

band from the excited normal form with O_8—H_8···O_9═C_9 structure (S_1 state), which undergoes an ESIPT process to the excited proton-transferred form with O_8···H_8—O_9—C_9 structure (S_1' state).[33] This process is ultrafast, and occurs within the time window limited by the instrument response function of the fluorescence up-conversion apparatus (<100 fs). Since the decay profiles (decay time and amplitude ratio) of the ultrafast decay components in methanol, EtOH, and 1-propanol are close to one another, the fast ESIPT process is probably not assisted by the solvent. The second decay component, whose decay time is ~500 fs, would come from solvent and molecular rearrangements that follow the ESIPT process, and the decay profile is also independent of alcohols. The long decay-time component in $\lambda \geq 570$ nm is $S_1' \rightarrow S_0'$ fluorescence of the proton-transferred form, because the rise is fast and has two time components of <100 fs and ~500 fs. Since the rates of the ESIPT and rearrangements are very fast, the normal form in the S_1 state of AS1 does not lead to harmful triplet photosensitization through intersystem crossing.

The solid curve in Figure 4 shows the $S_1' \rightarrow S_0'$ fluorescence decay of the proton-transferred AS1 monitored at 650 nm in

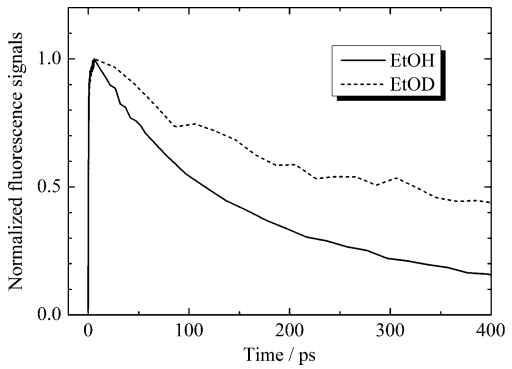

Figure 4. $S_1' \rightarrow S_0'$ fluorescence decays of proton-transferred AS1 monitored at 650 nm in EtOH and EtOD (solid and broken curves, respectively) at room temperature.

EtOH at room temperature. From the short fluorescence lifetime (170 ps), it is seen that fast $S_1' \rightarrow S_0'$ internal conversion prevents the harmful triplet photosensitization and causes UV protection as mentioned in the Introduction.

Deuterium kinetic isotope effects on the decay profile of AS1 were examined in EtOH and ethanol-d_1 (EtOD). The H atoms forming the intramolecular hydrogen bonds (H_3 and H_8) would be replaced by deuterons in EtOD.[41] In $\lambda \leq 520$ nm, the decay

dx.doi.org/10.1021/jp306870y | J. Phys. Chem. B 2013, 117, 4347−4353

profiles in EtOH and EtOD are close to each other. The deuterium kinetic isotope effect is negligible when the ESIPT process has no potential barrier along the reaction coordinate.[42] However, since the ESIPT process occurs within the time window limited by the instrument response function, it is unknown whether or not the kinetic isotope effect and a potential barrier are really absent in the ESIPT of AS1. Accordingly, we optimized the molecular structure in the ground state of a model for the normal form (Chart 2), and examined whether or not its local minimum causing a potential barrier in ESIPT is found in the lowest-excited $^1(\pi,\pi^*)$ state. On the potential surface of the lowest-excited $^1(\pi,\pi^*)$ state, the geometry optimization starting from the normal form led to the intramolecularly proton-transferred form shown in Chart 2. The absence of the local minimum of the normal form in the lowest-excited $^1(\pi,\pi^*)$ state suggests that the ESIPT process has no potential barrier, which is consistent with the nodal plane model.[19] The ultrafast $S_1 \rightarrow S_1'$ relaxation and the absence of the kinetic isotope effect found in our experimental results would be due to the absence of the potential barrier.

On the potential surface of the ground state, the geometry optimization starting from the intramolecularly proton-transferred form led to the normal form (Chart 2). Since a local minimum of the proton-transferred form is not found on the ground-state potential surface, the $S_0' \rightarrow S_0$ reverse proton-transfer process would also have no potential barrier along the reaction coordinate. Since the computational results given in Figure 1 satisfactorily reproduce the experimental electronic transition energies, effects of the solvent on the proton-transfer potential surfaces (for example, see ref 43) would be negligible.

In contrast to the decay profiles in $\lambda \leq 520$ nm, the long decay time in $\lambda \geq 570$ nm in EtOD (324 ps) is roughly twice as long as that in EtOH (170 ps), as shown in Figure 4. This large difference can be attributed to a kinetic isotope effect on the $S_1' \rightarrow S_0'$ internal conversion of the proton-transferred form. As mentioned in the Introduction,[23,24] out-of-plane bending and/or torsional motion around the $O_8\cdots X_8-O_9-C_9$ (X = H or D) moiety would play an important role in the fast internal conversion from the S_1' state, and therefore some kinetic isotope effects are reasonably expected in the decay from the S_1' state of the proton-transferred form.

Figure 5 shows some $S_1' \rightarrow S_0'$ fluorescence decays of the proton-transferred AS1 monitored at 600 nm in EtOH between 87 and 286 K. Each of the fluorescence decays is well characterized by a single exponential decay at all the temperatures (T), and the fluorescence lifetime is temperature dependent. For instance, at 286 K, the fluorescence lifetime is ~350 ps, and at 87 K, its value is ~610 ps. Figure 6a shows the temperature dependence of the fluorescence-decay rate constant $[k_f(T)]$. As in ESIPT-susceptible molecules studied previously,[24,44,45] $k_f(T)$ can be given by the sum of a temperature-dependent nonradiative decay rate constant $[k_f^{nr}(T)]$ and a temperature-independent decay rate constant (k_f^0).

$$k_f(T) = k_f^0 + k_f^{nr}(T) \quad (1)$$

k_f^0 comes from temperature-independent internal conversion, fluorescence, and intersystem crossing, and $k_f^{nr}(T)$ is likely to originate from temperature-dependent internal conversion.[18]

When k_f^0 is assumed to be 1.6×10^9 s^{-1}, $k_f^{nr}(T)$ shows the temperature dependency drawn in Figure 6b. The plot of log $k_f^{nr}(T)$ vs T^{-1} gives a satisfactory straight line. $k_f^{nr}(T)$ of ESIPT-susceptible molecules is known to be given approximately by[24,44,45]

$$k_f^{nr}(T) = k_f^{nr}(\infty) \exp(-E_a/RT) \quad (2)$$

where R, E_a, and $k_f^{nr}(\infty)$ denote the gas constant, an apparent activation energy, and a frequency factor, respectively. According to eq 2, E_a and $k_f^{nr}(\infty)$ can be estimated to be 4.7 ± 0.1 kJ/mol and $(8.4 \pm 0.3) \times 10^9$ s^{-1}, respectively, from Figure 6b. These values are not similar to those of *o*-hydroxypropiophenone (OHPP in Chart 3, E_a = 11 kJ/mol and $k_f^{nr}(\infty) = 1.6 \times 10^{12}$ s^{-1}) but close to those of 7-hydroxy-1-indanone (7HIN in Chart 3, E_a = 3.3 kJ/mol and $k_f^{nr}(\infty) = 2.0 \times 10^9$ s^{-1}).[24] In OHPP and 7HIN, the out-of-plane motion and/or torsional motion around the intramolecular hydrogen bond play an important role in the temperature-dependent fast internal conversion, and the presence of a rigid five-membered ring makes such a motion in 7HIN much more difficult than in OHPP. As a result, the internal conversion is drastically suppressed in 7HIN.[24] Similar suppression in $S_1' \rightarrow S_0'$ internal conversion may occur also in AS1 because the out-of-plane bending and/or torsional motion around the $O_8\cdots H_8-O_9-C_9$ moiety cause the internal conversion and the C_9 atom is a member of a rigid six-membered ring as in 7HIN. Such suppression in internal conversion may lower the UV protective activity of AS1. However, the rigid ring of AS1 may provide another advantage to aloe species and AS1 would in total contribute to their survival, because various intramolecularly hydrogen-bonded anthraquinones with such a rigid ring are found in aloe species.[17]

Figure 7 shows some $S_1' \rightarrow S_0'$ fluorescence decays of the proton-transferred AS1 monitored between 550 and 700 nm in EtOH at 160 K. As seen in the figure, the fluorescence lifetime is nearly independent of the monitoring wavelength. EtOH is a glass-forming liquid, and at 160 K, its dielectric relaxation is slower by 2.5 orders of magnitude than at room temperature.[46] In cases where solvation dynamics affects time-resolved emission, that of EtOH around a solute molecule at 160 K should be seen as a fast component of a few hundred picoseconds in the emission profile in a short wavelength range.[47] This is clearly not the case for AS1, because the fluorescence decays at all the monitored wavelengths are nearly identical to one another.

Some effects caused by addition of acid or base to the EtOD solution were examined on the AS1 fluorescence at room temperature. Although the effect of the acid addition on the spectrum was negligible, that of the base addition was clearly observed. The alternate long-and-short dashed curve in Figure

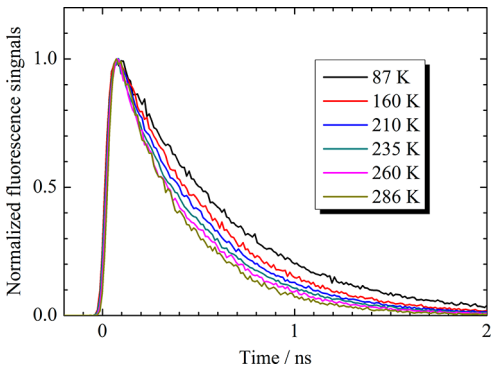

Figure 5. $S_1' \rightarrow S_0'$ fluorescence decays of proton-transferred AS1 monitored at 600 nm in EtOH between 87 and 286 K.

dx.doi.org/10.1021/jp306870y | J. Phys. Chem. B 2013, 117, 4347−4353

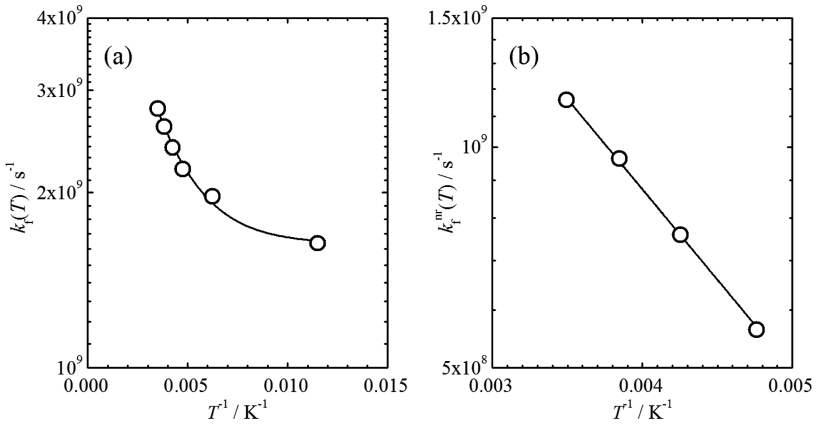

Figure 6. (a) Plot of log $k_f(T)$ vs T^{-1} for AS1 in EtOH. (b) Plot of log $k_f^{nr}(T)$ vs T^{-1} for AS1 in EtOH. The standard deviation of the rate constants is less than the size of the symbol.

Chart 3. Molecular Structures of *o*-Hydroxypropiophenone (OHPP) and 7-Hydroxy-1-indanone (7HIN)

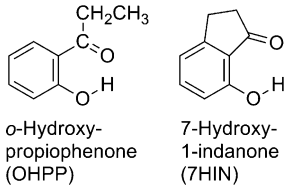

o-Hydroxy-propiophenone (OHPP)

7-Hydroxy-1-indanone (7HIN)

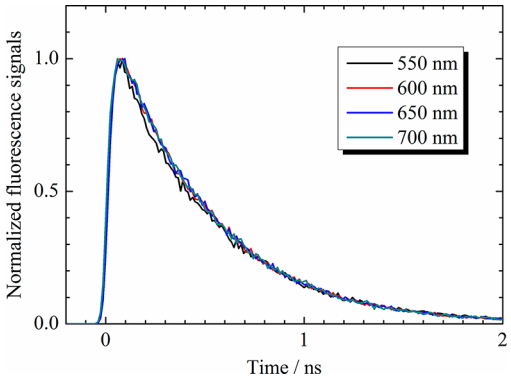

Figure 7. $S_1' \rightarrow S_0'$ fluorescence decays of proton-transferred AS1 monitored between 550 and 700 nm in EtOH at 160 K.

2 shows the fluorescence spectrum of AS1 in a basic EtOD solution. The fluorescence is red-shifted with a fluorescence peak at ~650 nm, and the intensity drops by more than an order of magnitude. This fact shows that the hydroxy proton at the 8-position (H_8) in the S_0 state dissociates in the basic solution, and the phenolate anion is formed as in 1-(acylamino)anthraquinones.[48] The hydroxy proton at the 3-position (H_3) may also dissociate. The deprotonated form shows very weak steady-state fluorescence. This may be due to a low transition dipole-moment (small oscillator strength). Another possibility is a nonradiative process (intersystem crossing, internal conversion, etc.) shortening the lifetime greatly, but any UV protective activity due to the nonradiative process may be absent in the deprotonated form insusceptible to ESIPT, as mentioned in the Introduction. Furthermore, the deprotonated AS1 in the basic solution may be degraded through an irreversible chemical reaction with $^1O_2$ that has been produced through triplet photosensitization of molecules other than AS1.[49] However, since human skin is kept weak acidic,[28] AS1 is not deprotonated there and the UV protective activity is kept on the skin. Furthermore, although Cleopatra liked bathing very much, she did not use alkaline soap but used body-scrubbing with white sand,[50] and so her UV protection would not have been prevented by some deprotonation of chemical constituents contained in aloe.

The hydroxy group at the 8-position in AS2 is, as in AS1, intramolecularly hydrogen-bonded to the carbonyl oxygen at the 9-position (O_8—H_8···O_9=C_9), but the hydroxy proton at the 3-position (H_3) is, in contrast to AS1, methylated and cannot be hydrogen-bonded to the adjacent carbonyl oxygen (Chart 1). As a result, ESIPT of H_3 is blocked in AS2. However, fluorescence decay curves of AS2 are close to those of AS1 at room temperature. This fact supports S.N.'s previous assertion that the ESIPT of AS1 takes place along only one of the molecule's two intramolecular hydrogen bonds (O_8—H_8···O_9=C_9).[33] The UV protective activity of AS1 would be induced by the ESIPT through O_8—H_8···O_9=C_9.

The hydroxy proton at the 8-position (H_8) in AS3 is, in contrast to AS1, methylated to block the ESIPT through O_8—H_8···O_9=C_9, but the hydroxy group at the 3-position in AS3 is, as in AS1, intramolecularly hydrogen-bonded to the carbonyl oxygen at the 2-position (O_3—H_3···O_2=C_2) (Chart 1). AS3 shows very weak steady-state fluorescence and the intensity drops by more than an order of magnitude on going from AS1 to AS3,[33] even though ESIPT of H_3 is not blocked. Although AS3 seems to show a fast decay of the fluorescence up-conversion signals in a long wavelength range at room temperature, the fluorescence may originate not from AS3 itself but from some impurity, dimer, oligomer, or so on. However, further measurements with improved signal-to-noise ratios are needed in a solvent in which AS3 really dissolves much more than in EtOH. It is interesting that methylsalicylate shows ESIPT,[51] whereas AS3, which is basically nothing more than a condensed-ring molecule to methylsalicylate with 5-methoxy-1,4-naphthoquinone, does not show characteristic fluorescence caused by ESIPT.

AS1 shows not only the UV protection but also the $^1O_2$ quenching activity, and electron-transfer from AS1 deactivates $^1O_2$ produced through triplet photosensitization of molecules other than AS1.[33] One advantage of AS1 as a $^1O_2$ quenching agent is its long lifetime due to its resistance to UV degradation, as mentioned in the Introduction. AS1 is not efficiently degraded by irreversible chemical reactions with reactive oxygen species ($^1O_2$ and free radicals), either.[33] Furthermore,

dx.doi.org/10.1021/jp306870y | J. Phys. Chem. B 2013, 117, 4347−4353

the $^1O_2$-quenching rate constant of AS1 is larger than that of vitamin E (α-tocopherol) that is well-known as an efficient $^1O_2$ quencher.[52,53] AS1 forms a stable encounter complex with $^1O_2$ ($\{AS1\cdots{}^1O_2\}$), and the O_8—H_8···O_9=C_9 moiety participating in ESIPT plays an important role also in the $^1O_2$ quenching through the complex formation.[33] On the basis of the present results, the reason for the coexistence of the UV protection (ESIPT) and $^1O_2$ quenching activity in AS1 could be qualitatively explained in the following way.

When an intramolecular hydrogen bond causing ESIPT is absent as in anthraflavic acid (2,6-dihydroxyanthraquinone) found in rhubarb (an ancient Chinese herbal medicine),[54] the potential surfaces of the S_0 and S_1 states are basically similar to each other (Figure 8a-1). In contrast, the very fast ESIPT and

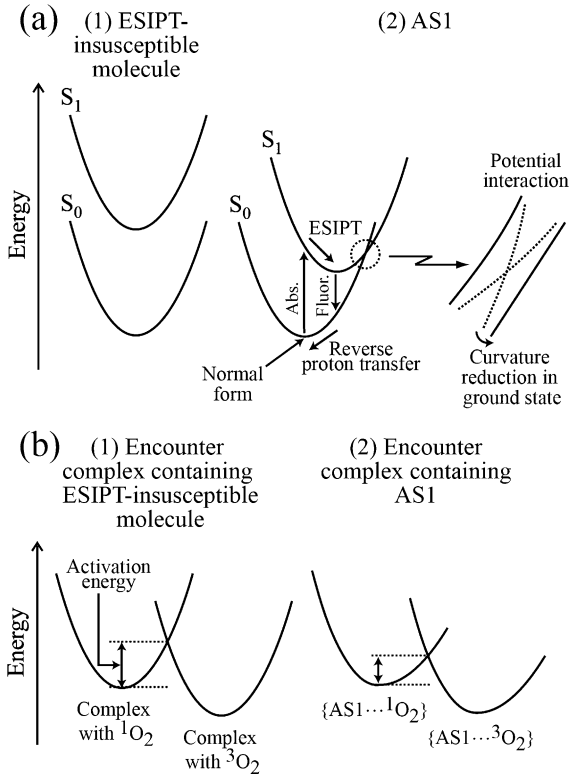

Figure 8. Schematic representation of potential curves of an ESIPT-insusceptible molecule (a-1), AS1 (a-2), and their encounter complexes with $^{1,3}O_2$ (b-1 and b-2).

$S_1' \rightarrow S_0'$ internal conversion observed this time in AS1 suggest that the potential surfaces of the S_0 (S_0') and S_1 (S_1') states interact with each other, as shown in Figure 8a-2, and the ESIPT reduces the potential surface curvature of the S_0 (S_0') state (Figure 8b-2). Thus, the activation energy of the $^1O_2 \rightarrow {}^3O_2$ quenching in the encounter complex containing ESIPT-susceptible AS1 (Figure 8b-2) is less than in a complex containing ESIPT-insusceptible molecule (Figure 8b-1) or than in the case that the sample does not form a stable encounter complex with $^1O_2$. As a result, ESIPT-active and UV-protective AS1 is considered to show the high $^1O_2$-quenching activity. The transition state between $\{AS1\cdots{}^1O_2\}$ and $\{AS1\cdots{}^3O_2\}$ in Figure 8b-2 would have properties of partial electron transfer from the O_8—H_8···O_9=C_9 moiety to $^1O_2$. In intramolecularly hydrogen-bonded anthraquinones, UV protective activity provided by ESIPT linearly correlates with $^1O_2$ quenching activity.[34] The quenching-reaction coordinate from $\{AS1\cdots{}^1O_2\}$ to $\{AS1\cdots{}^3O_2\}$ would have a component parallel to the reaction coordinate of ESIPT.

It is regrettable that the content of AS1 in aloe and the molecular concentration in solutions extracted from aloe have not yet been reported, but we may assume that the molecular concentration of AS1 in a solution extracted from aloe is similar to that of aloe-emodin (1.0×10^{-4} M).[55] Then, since the molecular absorption coefficient (ε) of AS1 in EtOH (Figure 2) is 3000−17 000 L $mol^{-1}cm^{-1}$ in the region of UV shining on the earth surface (290−400 nm),[28c] the absorbance for 1 cm is 0.3−1.7, and thus fair UV protection is expected from AS1 alone. Various intramolecularly hydrogen-bonded molecules present in aloe besides AS1 would jointly provide the UV protective function of aloe.

5. SUMMARY

Time-resolved emission of AS1 was studied with the fluorescence up-conversion and TCSPC techniques. The rates of the ESIPT, of the solvent and molecular rearrangements, and of the decay from the S_1' state were determined and interpreted in light of TDDFT calculations. These results were discussed in conjunction with UV protection and $^1O_2$ quenching activity of aloe. Since the rates observed are very fast, AS1 does not lead to harmful triplet photosensitization through intersystem crossing. The TDDFT-calculation results are consistent with the experimental ones, and the ESIPT and reverse proton-transfer processes are barrierless along the reaction coordinates in the lowest-excited $^1(\pi,\pi^*)$ and ground states, respectively. Out-of-plane bending and/or torsional motion around the $O_8\cdots H_8$—O_9—C_9 moiety play an important part in temperature-dependent fast $S_1' \rightarrow S_0'$ internal conversion and have a deuterium kinetic isotope effect on it. Solvation dynamics does not affect the time-resolved emission. In a basic solution, the H_8 proton dissociates in the S_0 state, and so the fluorescence is red-shifted and its intensity drops. The substituent effect seen in the time-resolved emission of AS1, AS2, and AS3 supports S.N.'s previous assertion that the ESIPT of AS1 takes place along only one of the molecule's two intramolecular hydrogen bonds (O_8—H_8···O_9=C_9).

■ ASSOCIATED CONTENT

Ⓢ Supporting Information

Fluorescence rise-and-decay signals of AS1, AS2, and AS3, $S_1' \rightarrow S_0'$ fluorescence lifetimes of AS1 at various temperatures, optimized structures in the ground and lowest-excited $^1(\pi,\pi^*)$ states of models for AS1 at the time-dependent B3LYP/6-311G**//LC-BLYP/6-311G** level, and computational results of the models at the time-dependent LC-BLYP/6-311G**//B3LYP/6-311G** level. This material is available free of charge via the Internet at http://pubs.acs.org.

■ AUTHOR INFORMATION

Corresponding Author

*Phone: 972-3-6407012. Fax: 972-3-6407491. E-mail: huppert@tulip.tau.ac.il.

Notes

The authors declare no competing financial interest.

■ ACKNOWLEDGMENTS

S.N. thanks Miss Kanako Fujita of Ehime University for her kind help in the sample preparation and thanks Dr. Umpei Nagashima of Japanese National Institute of Advanced

Industrial Science and Technology and Professor Hiroyuki Teramae of Josai University for their valuable discussion on ESIPT, $^1O_2$ quenching, and TDDFT calculations of AS1. S.N. is also grateful to Lecturer Yasuko Hatamori of Ehime University for her advice on ancient Egypt. This work was partly supported by Grants-in-Aid from the James-Franck German-Israeli Program in Laser-Matter Interaction and from the Israel Science Foundation to D.H., and also by a Grant-in-Aid for Challenging Exploratory Research (No. 24658123) from Japan Society for the Promotion of Science to S.N.

REFERENCES

(1) Grindlay, D.; Reynolds, T. *J. Ethnopharmacol.* **1986**, *16*, 117−151.
(2) Haller, J. S., Jr. *Bull. N.Y. Acad. Med.* **1990**, *66*, 647−659.
(3) Reynolds, T.; Dweck, A. C. *J. Ethnopharmacol.* **1999**, *68*, 3−37.
(4) Kemper, K. J.; Chiou, V. Aloe Vera, http://www.longwoodherbal.org/aloe/aloe.pdf (accessed Nov 2012) and references cited therein.
(5) Eshun, K.; He, Q. *Crit. Rev. Food Sci. Nutr.* **2004**, *44*, 91−96.
(6) Atherton, P. *Nurs. Stand.* **1998**, *12*, 49−54.
(7) Strouhal, E. *Life in Ancient Egypt*; Opus/Cambridge University Press: London, 1992; Chapter 7.
(8) Bianchi, R. S. Cleopatra. In *The Oxford Encyclopedia of Ancient Egypt*; Redford, D. B., Ed.; Oxford University Press: New York, 2001; Vol. *1*. Although BBC News (http://news.bbc.co.uk/2/hi/uk_news/scotland/tayside_and_central/7958819.stm, accessed Nov 2012) reported that Arsinoe (a half-sister to Cleopatra, having a different mother) had had both European and ancient Egyptian characteristics judging from a skull and a skeleton found in Ephesus (Turkey), the skull and skeleton are not proven to be those of Arsinoe.
(9) Heller, H. J. *Eur. Polym. J. Suppl.* **1969**, 105−132.
(10) Aloui, F.; Ahajji, A.; Irmouli, Y.; George, B.; Charrier, B.; Merlin, A. *Appl. Surf. Sci.* **2007**, *253*, 3737−3745.
(11) Barbara, P. F.; Walsh, P. K.; Brus, L. E. *J. Phys. Chem.* **1989**, *93*, 29−34.
(12) Formosinho, S. J.; Arnaut, L. G. *J. Photochem. Photobiol., A* **1993**, *75*, 21−48.
(13) Sugawara, T.; Takasu, I. *Adv. Phys. Org. Chem.* **1999**, *32*, 219−265.
(14) Chou, P.-T. *J. Chin. Chem. Soc.* **2001**, *48*, 651−682.
(15) Nagaoka, S.; Teramae, H.; Nagashima, U. *Bull. Chem. Soc. Jpn.* **2009**, *82*, 570−573 and references cited therein..
(16) Turro, N. J.; Ramamurthy, V.; Scaiano, J. C. *Modern Molecular Photochemistry of Organic Molecules*; University Science Books: Herndon, VA, 2010; Section 5.19.
(17) Dagne, E.; Bisrat, D.; Viljoen, A.; Van Wyk, B.-E. *Curr. Org. Chem.* **2000**, *4*, 1055−1078.
(18) Stock, K.; Bizjak, T.; Lochbrunner, S. *Chem. Phys. Lett.* **2002**, *354*, 409−416.
(19) Nagaoka, S.; Nagashima, U.; Ohta, N.; Fujita, M.; Takemura, T. *J. Phys. Chem.* **1988**, *92*, 166−171.
(20) Nagaoka, S.; Nagashima, U. *Chem. Phys.* **1996**, *206*, 353−362.
(21) Paul, B. K.; Samanta, A.; Guchhait, N. *Photochem. Photobiol. Sci.* **2010**, *9*, 57−67 and references cited therein..
(22) Park, S.; Kwon, J. E.; Park, S. Y. *Phys. Chem. Chem. Phys.* **2012**, *14*, 8878−8884.
(23) Barbara, P. F.; Brus, L. E.; Rentzepis, P. M. *J. Am. Chem. Soc.* **1980**, *102*, 5631−5635.
(24) Nagaoka, S.; Hirota, N.; Sumitani, M.; Yoshihara, K.; Lipczynska-Kochany, E.; Iwamura, H. *J. Am. Chem. Soc.* **1984**, *106*, 6913−6916.
(25) Williams, D. L.; Heller, A. *J. Phys. Chem.* **1970**, *74*, 4473−4480.
(26) Hussein, Y. H. A.; Anderson, N.; Lian, T. T.; Abdou, I. M.; Strekowski, L.; Timoshchuk, V. A.; Vaghefi, M. M.; Netzel, T. L. *J. Phys. Chem. A* **2006**, *110*, 4320−4328 (see the first paragraph of the right column in p 4321).
(27) Hubig, S. M.; Bockman, T. M.; Kochi, J. K. *J. Am. Chem. Soc.* **1997**, *119*, 2926−2935.
(28) *New Cosmetic Science*; Mitsui, T., Ed.; Elsevier: Amsterdam, The Netherlands, 1997. *Shin-Kesyouhingaku*, 2nd ed.; Nanzando: Tokyo, 2001; Part I: (a) Section 5.5, (b) Section 1.2, (c) Section 1.6.
(29) Stein, M.; Keck, J.; Waiblinger, F.; Fluegge, A. P.; Kramer, H. E. A.; Hartschuh, A.; Port, H.; Leppard, D.; Rytz, G. *J. Phys. Chem. A* **2002**, *106*, 2055−2066.
(30) Yagi, A.; Makino, K.; Nishioka, I. *Chem. Pharm. Bull.* **1974**, *22*, 1159−1166.
(31) Uno, H.; Nagamachi, Y.; Honda, E.; Masumoto, A.; Ono, N. *Chem. Lett.* **2000**, 1014−1015.
(32) Uno, H.; Masumoto, A.; Honda, E.; Nagamachi, Y.; Yamaoka, Y.; Ono, N. *J. Chem. Soc., Perkin Trans. 1* **2001**, 3189−3197.
(33) Nagaoka, S.; Fujii, A.; Hino, M.; Takemoto, M.; Yasuda, M.; Mishima, M.; Ohara, K.; Masumoto, A.; Uno, H.; Nagashima, U. *J. Phys. Chem. B* **2007**, *111*, 13116−13123; ibid **2012**, *116*, 2338.
(34) Nagaoka, S.; Ohara, K.; Takei, M.; Nakamura, M.; Mishima, M.; Nagashima, U. *J. Photochem. Photobiol., A* **2011**, *225*, 106−112; ibid **2012**, *240*, 75.
(35) Erez, Y.; Presiado, I.; Gepshtein, R.; Huppert, D. *J. Phys. Chem. A* **2012**, *116*, 2039−2048.
(36) Erez, Y.; Gepshtein, R.; Presiado, I.; Trujillo, K.; Kallio, K.; Remington, S. J.; Huppert, D. *J. Phys. Chem. B* **2011**, *115*, 11776−11785.
(37) Teramae, H.; Nagaoka, S.; Nagashima, U. *Int. J. Chem. Model.*, in press.
(38) Yu, X.-f.; Yamazaki, S.; Taketsugu, T. *J. Chem. Theory Comput.* **2011**, *7*, 1006−1015.
(39) Krishnan, R.; Binkley, J. S.; Seeger, R.; Pople, J. A. *J. Chem. Phys.* **1980**, *72*, 650−654.
(40) Frisch, M. J.; Trucks, G. W.; Schlegel, H. B.; Scuseria, G. E.; Robb, M. A.; Cheeseman, J. R.; Scalmani, G.; Barone, V.; Mennucci, B.; Petersson, G. A.; Nakatsuji, H.; et al. *Gaussian 09*, revision C.01; Gaussian, Inc.: Wallingford, CT, 2010.
(41) Nagaoka, S.; Kuranaka, A.; Tsuboi, H.; Nagashima, U.; Mukai, K. *J. Phys. Chem.* **1992**, *96*, 2754−2761.
(42) Bell, R. P. *The Tunnel Effect in Chemistry*; Chapman and Hall: London, 1980; Chapter 4.
(43) Mukherjee, M.; Bandyopadhyay, B.; Chakraborty, T. *Chem. Phys. Lett.* **2012**, *546*, 74−79.
(44) Smith, K. K.; Kaufmann, K. J. *J. Phys. Chem.* **1978**, *82*, 2286−2291.
(45) Nagaoka, S.; Hirota, N.; Sumitani, M.; Yoshihara, K. *J. Am. Chem. Soc.* **1983**, *105*, 4220−4226.
(46) Stickel, F. J. Ph.D. Dissertation, University of Mainz (D77), 1995.
(47) Papazyan, A.; Maroncelli, M. *J. Chem. Phys.* **1995**, *102*, 2888−2919.
(48) Smith, T. P.; Zaklika, K. A.; Thakur, K.; Walker, G. C.; Tominaga, K.; Barbara, P. F. *J. Phys. Chem.* **1991**, *95*, 10465−10475.
(49) Bisby, R. H.; Morgan, C. G.; Hamblett, I.; Gorman, A. A. *J. Phys. Chem. A* **1999**, *103*, 7454−7459.
(50) Bramson, A. S. *Soap-Making It, Enjoying It*; Workman: New York, 1972.
(51) Nagaoka, S.; Nakamura, A.; Nagashima, U. *J. Photochem. Photobiol., A* **2002**, *154*, 23−32 and references cited therein.
(52) Schweitzer, C.; Schmidt, R. *Chem. Rev.* **2003**, *103*, 1685−1757 and references cited therein.
(53) Mukai, K.; Itoh, S.; Daifuku, K.; Morimoto, H.; Inoue, K. *Biochim. Biophys. Acta* **1993**, *1183*, 323−326.
(54) Zhang, H.-X.; Liu, M.-C. *J. Chromatogr., B* **2004**, *812*, 175−181.
(55) Conner, J. M.; Gray, A. I.; Waterman, P. G.; Reynolds, T. *J. Nat. Prod.* **1990**, *53*, 1362−1364.